Degree of polarization as an objective method of estimating scattering

Juan M. Bueno, Esther Berrio, Maris Ozolinsh,* and Pablo Artal

Laboratorio de Óptica, Departamento de Física, Universidad de Murcia, Campus de Espinardo (Edificio C), 30071 Murcia, Spain

Received September 16, 2003; revised manuscript received January 8, 2004; accepted March 12, 2004

A new method of determining objectively the amount of scattered light in an optical system has been developed. It is based on measuring the degree of polarization of the light in images formed after a double pass through the system. A dual apparatus composed of a modified double-pass imaging polarimeter and a wave-front sensor was used to measure polarization properties and aberrations of the system under test. We studied the accuracy of the procedure in a system that included a lanthanum-modified lead zirconate titanate (PLZT) ceramic plate able to generate variable amounts of scattered light as a function of the applied voltage. Changes in the voltage applied to the ceramics plate modified significantly the scattering contribution while hardly altering the wave-front aberration. The degree of polarization was well correlated with the level of scattering in the system as determined by direct-intensity measurements at the tails of the double-pass images. This indicates that this polarimetric parameter provides accurate relative estimates of the amount of scattering generated in a system. The technique can be used in a number of applications, for example, to determine objectively the amount of scattered light in the human eye. © 2004 Optical Society of America

OCIS codes: 290.0290, 120.5820, 120.5410, 220.4840.

1. INTRODUCTION

Under most conditions aberrations are the chief cause of degradation of the images formed by optical systems. However, there is another important factor that contributes at some level to degrading of the quality of an optical system: scattered light.

Since scattering reduces the contrast of the images, estimation of the amount of scattering and, eventually, any improvement in observing objects through scattering media are challenging tasks in applications such as atmospheric remote sensing, underwater photography, microscopy, optical coherence techniques, and medical imaging. In particular, imaging techniques in astronomy and visual optics, which are based on observing through the atmosphere and through the ocular media, respectively, are interesting examples of systems limited by both aberrations and scattering. In the case of the human eye, beyond aberrations, intraocular scattering[1,2] reduces the contrast of retinal images, thus lowering visual performance. Scattering is low in young, healthy eyes but becomes larger with aging and some pathologies. Although robust techniques have been developed to measure aberrations in different environments,[3–5] a consistent method of objectively evaluating the contribution of scattered light has not yet been reported.

It is well known that changes in polarization of incident light are correlated with the scattering properties of the media. To that end, various previous studies have combined measurement of light intensity as a function of the angle (scatterometry) with polarimetric techniques to extract information on the properties of surfaces or scattering media.[6–9]

In this paper we propose a new procedure to estimate differences in the amount of scattered light. Since depolarization is a property intrinsically associated with scattering and the loss of coherence in the polarization state,[10] we have evaluated the possibility of using the degree of polarization (DOP) of the light passing through a system as a parameter to quantify scattering in the presence of aberrations. In this sense, changes in the amount of scattered light would be related to changes in the DOP of the light caused by its propagation through the system. The procedure requires polarimetric measurements on the image of a point source formed by the system. In many practical cases, and in particular in the human eye, there is no direct access to the image plane so a double-pass (DP) configuration was adopted.[11,12] The reliability of the proposed technique has been tested in a system similar to an artificial eye that incorporates an electro-optical ceramic plate[13] that produces a variable amount of light scattering.

2. METHODS

A. Apparatus

Figure 1 shows a schematic diagram of the experimental system used in this paper. The apparatus is based on a DP imaging polarimeter previously described.[14] A collimated green laser beam (543-nm wavelength and 1-mm diameter) is used to generate a beacon light source on the focal plane of the system under study in the first passage. A linear polarizer P1 in the entrance path acts as the polarization-state generator unit, transmitting only vertically polarized light toward the sample. In the second passage, the reflected light is transmitted by a pellicle beam splitter BS, propagates through a focus corrector system FC, then through the polarization-state analyzer unit AU, and reaches a cooled, scientific-grade, slow-scan

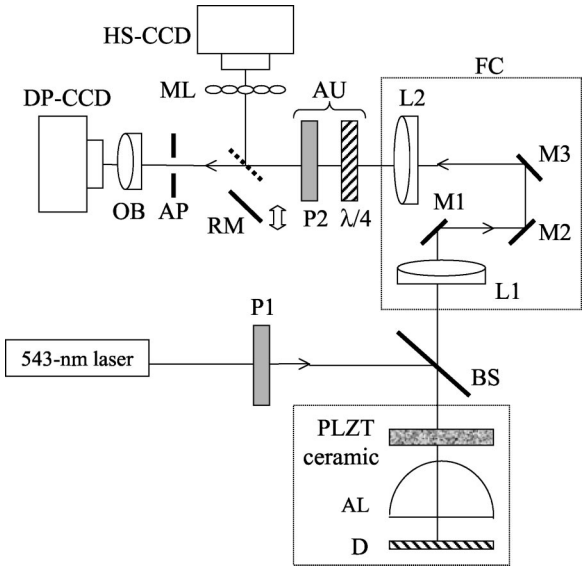

Fig. 1. Schematic diagram of the experimental apparatus (see text for details).

CCD camera DP-CCD provided with a 50-mm objective OB. The FC consists of a pair of achromatic doublets L1 and L2, with 190- and 200-nm focal lengths, respectively, separated by three mirrors, two of them, M2 and M3 placed on a scaled moving stage to modify the optical pathway between the two lenses in order to correct defocus. The AU is composed of a rotating λ/4 plate and a fixed linear polarizer P2 with its transmission axis parallel to that of P1. Both elements in the AU can be removed independently from the system when necessary. Moreover, P2's transmission axis can be oriented at different angles. A 5-mm aperture AP placed in a plane conjugated to the sample's pupil acts as the effective exit pupil.

Additionally, a removable mirror RM oriented at 45° with respect to the optical axis is used to modify the registration pathway to record Hartmann–Shack (HS) images,[4,15] and also to measure the aberrations of the system under study. For this configuration, L1 and L2 conjugate the pupil's plane with the microlens array, ML, of 45-mm focal length and with a 0.6-mm single microlens aperture, that samples the emerging wave front. A second cooled, scientific-grade CCD camera, HS-CCD, is used to record the HS images.

The system used to test the procedure consists of three parts: a 25.4-mm flat–convex lens AL, a rotating diffuser D placed at the focal plane of AL, and an electro-optical lanthanum modified lead zirconate titanate (PLZT) ceramic plate[13] that permits generation of controlled amounts of scattering. The testing system is mounted on a three-dimensional micrometric translation stage to facilitate its alignment.

PLZT ceramics are transparent, ferroelectric materials that generate different scattering levels when the applied voltage is changed. When an electrical field is applied to the transparent electrodes deposited on both opposite sides of a PLZT plate (1.5 mm in thickness), reversible nucleations of submicrometer-size, dielectrically polar and birefringent regions are induced that produce local variations of the refractive index of the ceramic material. This produces an amount of forward stray light that increases with voltage. As an example, Fig. 2 shows images of an object taken directly through the ceramic sample for two different scattering levels (600 and 1100 V). The circular shape of the illuminated area is produced by the aperture of the ceramic holder. The visual effect caused by an increase in scattering is quite evident in Fig. 2(b). It exhibits a kind of foggy appearance but still keeps some information on small features. It should also be pointed out that the PLZT plate introduces a small amount of scattering even when no voltage is applied; that is, the medium is not totally transparent in the absence of an applied voltage.

B. Experimental Procedure

The protocol carried out for measurements is explained in the following. First, HS images of the system were recorded for different scattering levels (for this operation the AU was removed from the setup). The wave-front aberrations (WAs) were reconstructed from these measurements. The procedure to estimate aberrations from HS images has been extensively described elsewhere.[15] The WAs were estimated for a 5-mm pupil diameter and expressed as a series of Zernike coefficients[16] up to the 6th order. The rms wave-front error (i.e., the deviation of the wave front from an ideal surface) was used as an overall image quality parameter. This is defined as the square root of the sum of the squares of all Zernike coefficients.

In the second part of the experiment, RM was removed from the registration pathway in order to record "standard" DP images for different levels of scattering. Afterward, the P2 linear polarizer was included in the exit branch of the apparatus with its transmission axis oriented in the horizontal direction. DP images for crossed linear polarizers were recorded for the same scattering levels.

Finally, the λ/4 plate was added to the setup and a series of four "polarimetric" DP images were recorded for every scattering level. Each image in the series corresponded to an independent polarization state in the AU. These states were produced by orienting the fast axis of the λ/4 plate at four different angles[17]: −45°, 0°, 30°, and 60°.

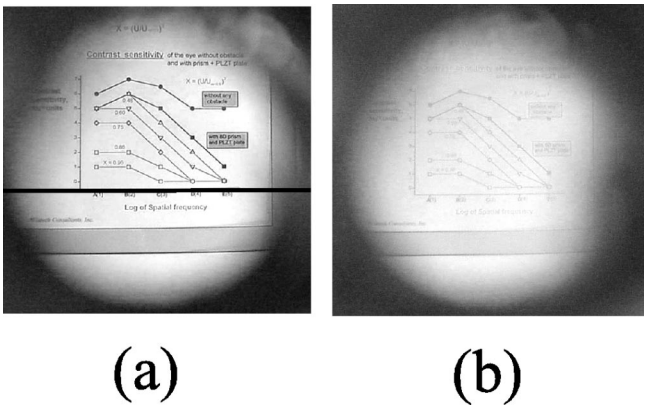

Fig. 2. Example of images of an object seen through the PLZT ceramic material for two different applied voltages: (a) 600 V, (b) 1100 V.

Every DP image subtended a field of 5.5° and its averaged radial profile was computed. To emphasize possible differences in the tails of the images due to changes in scattering, a parameter k' was computed as the area under the DP-intensity radial profile between 50 and 110 arc min. This range was adopted by assuming that the contribution of scattered light at these parts of the images should predominate over the effect of low- and mid-order aberrations. On the other hand, the degree of polarization was computed from the four polarimetric DP images as explained below.

C. Calculation of the Degree of Polarization

In this section we describe how the DOP was calculated. Let $\mathbf{S}_{\mathrm{OUT}}$ be the 4×1 emergent Stokes vector. If M_{PSA} is an auxiliary 4×4 matrix with each row being the first row of every Mueller matrix corresponding to an independent polarization state in the AU, then it is verified that

$$\begin{pmatrix} I_1 \\ I_2 \\ I_3 \\ I_4 \end{pmatrix} = \frac{1}{2}\begin{bmatrix} 1 & 0 & 0 & -1 \\ 1 & -1 & 0 & 0 \\ 1 & -1/4 & -\sqrt{3}/4 & \sqrt{3}/2 \\ 1 & -1/4 & \sqrt{3}/4 & \sqrt{3}/2 \end{bmatrix}\begin{pmatrix} S_0 \\ S_1 \\ S_2 \\ S_3 \end{pmatrix} = M_{\mathrm{PSA}} \cdot \mathbf{S}_{\mathrm{OUT}}, \tag{1}$$

where I_j $(j = 1, 2, 3, 4)$ are the intensities at each pixel in the DP images registered for each orientation of the fast axis in the $\lambda/4$ plate. The four elements of the Stokes vector $\mathbf{S}_{\mathrm{OUT}}$ can be calculated by inversion of Eq. (1) as

$$\mathbf{S}_{\mathrm{OUT}} = \begin{pmatrix} S_0 \\ S_1 \\ S_2 \\ S_3 \end{pmatrix} = (M_{\mathrm{PSA}})^{-1}\begin{pmatrix} I_1 \\ I_2 \\ I_3 \\ I_4 \end{pmatrix}. \tag{2}$$

This vector contains information on the polarization properties of the system under test, including the effects of depolarization. In particular, the DOP, defined as the ratio of the polarized-component intensity to the total intensity, can be directly computed from Eq. (2) as

$$\mathrm{DOP} = \frac{(S_1^{\,2} + S_2^{\,2} + S_3^{\,2})^{1/2}}{S_0}. \tag{3}$$

The DOP ranges from 0 (depolarized light) to 1 (totally polarized light). Values within this range correspond to partially polarized light.

D. Calibration

Before performing the complete study as a function of the level of scattering, we performed a simple calibration process. The PLZT plate was removed and a series of four DP images were recorded to test the system (AL + D), one for each adequate orientation of the $\lambda/4$ plate. Without the ceramic, the system should hardly change the DOP of the incoming polarization state (DOP = 1). Applying the procedure described above, the Stokes vector of the light was reconstructed and the corresponding DOP calculated by means of Eqs. (2) and (3). The value of the DOP obtained at the core of the image was 0.943. This result confirms the reliability of the apparatus and provides an offset value for the DOP estimation in our procedure.

3. RESULTS

The DP image formed by a system contains information on both aberrations and scattering. Whereas the aberrations are assumed to affect predominantly the relative shape of the central part of the image, scattered light contributes mainly to the tails. However, both factors together affect the image quality, and it is quite difficult to separate out their exact contributions. In particular, scattering is often explained as the contribution of extremely high-order aberrations.

Since the scattering introduced by the PLZT ceramic plate is due to local changes in the refractive index, and this also induces local phase changes, it is important to know the amount and type of aberrations produced by the sample as the voltage is varied. This will allow us to determine whether any significant change detected in the light-intensity distribution of the DP image is due to the isolated effect of a variation in light scattering or to a combined effect of variations in scattering and aberrations.

For this purpose, HS images of the system under test were recorded for four different scattering levels (those produced when applying 0, 600, 800, and 1000 V) with the AU not included in the apparatus. Figure 3 shows the corresponding mean values and standard deviations of the Zernike coefficients of the WA for a 5-mm pupil diameter (from the 2nd to the 5th order) estimated for the scattering levels. The small error bars obtained indicate that the ceramic plate does not induce a significant amount of additional aberrations when it is driven with high voltages, rendering it primarily a scattering generator. To better illustrate the effect of the applied voltage on the aberrations profile, Fig. 4 shows the WAs and the associated point-spread functions (PSFs) for these four different applied voltages. The rms wave-front error varies slightly, from 0.43 to 0.48 μm, as the voltage is increased from 0 to 1000 V.

A redistribution of the light intensity in the DP image occurs when the volume of scattered light increases, in

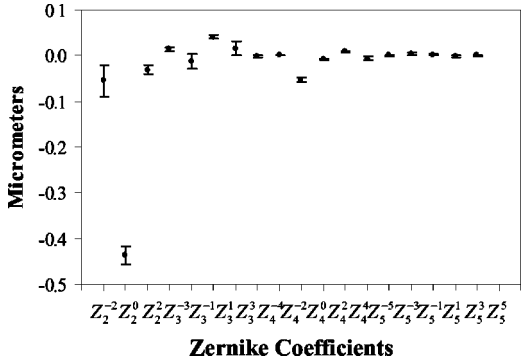

Fig. 3. Mean values of Zernike coefficients (in micrometers) from the 2nd to the 5th order, corresponding to the WAs for four different scattering levels generated by the ceramic plate. The pupil diameter was 5 mm; error bars represent ± 1 standard deviation.

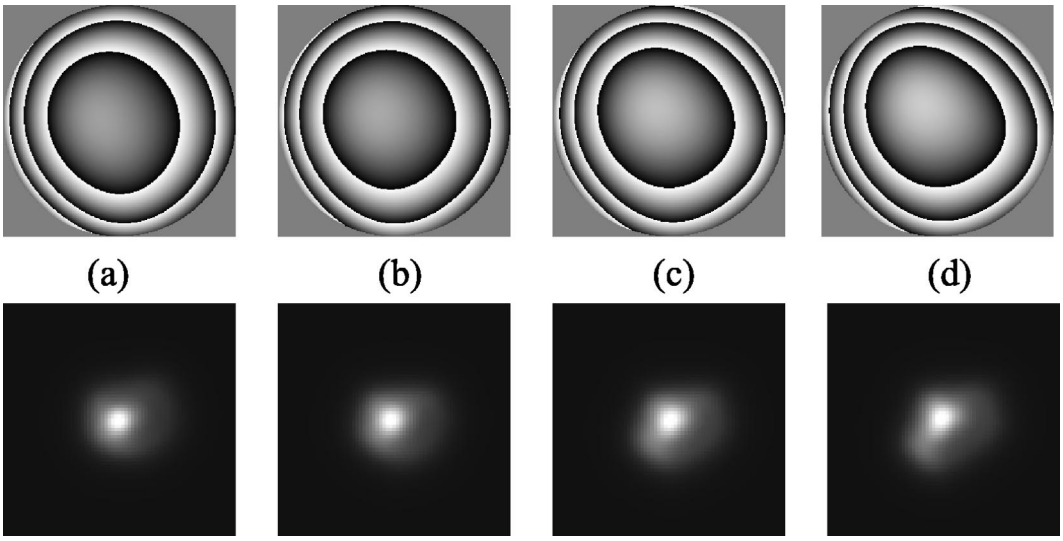

Fig. 4. WAs (upper panels) and associated PSFs (lower panels) for four scattering levels: (a) 0, (b) 600, (c) 800, and (d) 1000 V and a 5-mm pupil diameter. Each PSF subtends 25.8 arc min.

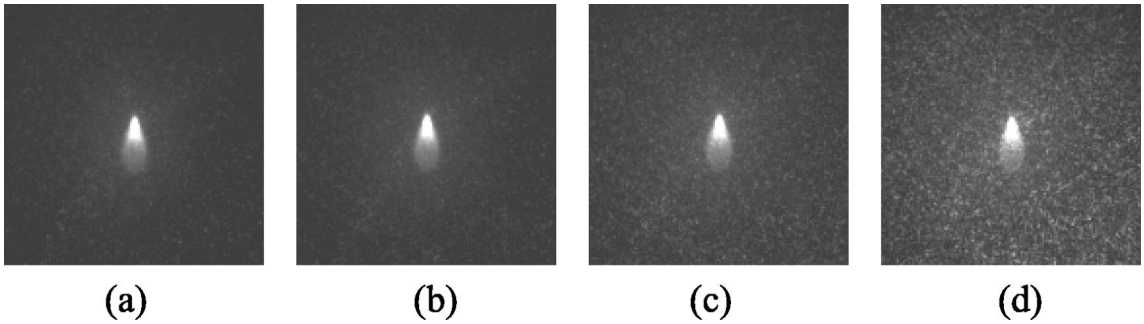

Fig. 5. DP images recorded for the same values of voltage as in Fig. 4. The contrast of the images has been modified to improve the visualization of the tails. Each image subtends 2.9°.

such a way that the maximum intensity (the peak) in the images decays whereas the amount of light in the tails becomes higher. These two effects are closely related to an image quality reduction and a net decrease of the optical performance, and are illustrated in Figs. 5 and 6.

Figure 5 shows the DP images corresponding to the previous scattering levels. Each image subtends 2.9° of angular field. The contrast of these images has been enhanced for a better visualization of the light distribution beyond the center. A direct visual inspection reveals an increment in the amount of light intensity in the tails of the images for larger voltages, and this is associated with an increase in scattered light. On the other hand, Fig. 6 shows the radial profiles for different DP images (up to 4° and centered on the peak value) within the range 600–1200 V. The curve for 0 V is also included as a reference. For higher applied voltages the intensity at the peak of the DP images decreases (upper panel), while the amount of light in the outer area increases (bottom panel), as is expected for a growing density of scattering sources.

The intersection point of all the DP radial profiles is located away from the center (maximum value) and closer than 50 arc min. Accordingly, we proposed to calculate a parameter k' as the area under the DP radial curve in the range from 50 to 110 arc min as an adequate estimator of the scattering contribution. Figure 7 presents the variation of k' as a function of the voltage applied to the PLZT ceramic plate. The parameter k' increases with voltage with a behavior well described by a second-order polynomial function (regression coefficient $R^2 = 0.9933$ and variance $p = 0.0006$). This is in agreement with the quadratic dependence between the induced birefringence and the applied voltage of the electric field, found empirically for this type of material.[13]

From the polarimetric DP images, the Stokes vector at each point in the radial profile was reconstructed. From this vector the DOP was calculated at each radial location of the DP image. Figure 8 shows the DOP profiles for the different scattering levels. The DOP at the center of the image clearly decreases with the eccentricity, owing to light-scattering. To ensure a more robust dependence on scattering, the DOP was computed by using the Stokes vector reconstructed from the averaged intensities over a small circular area (2.6 arc min in diameter) around the maximum value in the DP images. The feasibility of using this "averaged DOP" to estimate scattering was then analyzed by plotting it against the k' values of the DP images for a series of scattering levels (Fig. 9). In this case, the DP images were recorded with crossed polarizers in the first and second passes. With this particular configuration the filtering of the light that has not been scattered by the system is more effective (which is especially impor-

tant in analyzing the tails), although at the price of lowering the signal-to-noise ratio. The two parameters showed a good negative linear correlation ($R^2 = 0.9389, p = 0.0014$) with higher values of k' corresponding to lower values of the DOP. Since the light in the tails is mainly depolarized, this configuration ensures that k' quantifies essentially the scattering component; thus this result supports the use of the DOP parameter as a powerful tool for characterizing the relative amount of scattered light generated.

Finally, since aberrations modify the central part of the DP images, it might be possible that the estimates of the DOP would somehow be influenced by aberrations. If this were the case, our method would not be sufficiently robust to measure light scattering. To evaluate this possibility, we computed the DOP under the same conditions of scattering but for different amounts of defocus induced in the system. For this purpose, polarimetric DP images were recorded for the best focus and for four different defocus positions: $\pm 0.55\ D$ and $\pm 0.275\ D$. In all those cases, the values for the DOP were quite similar: The mean value ($\pm$ standard deviation) at the core of the images was 0.89 ± 0.01. The small changes in the DOP with defocus indicate that the proposed method is essentially unaffected, at least by moderate changes in aberrations.

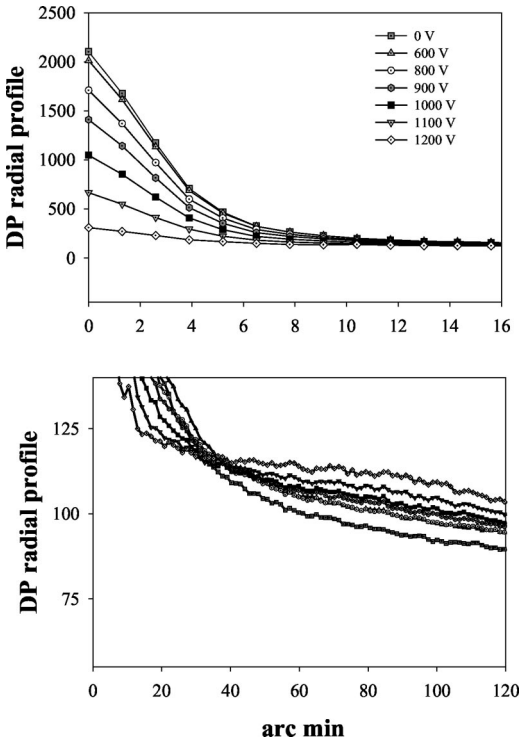

Fig. 6. Intensity radial profiles corresponding to the DP images as a function of voltage. The upper panel focuses on the region around the maximum peak of the images while the lower panel is scaled to show better the intensity at the tails of the images.

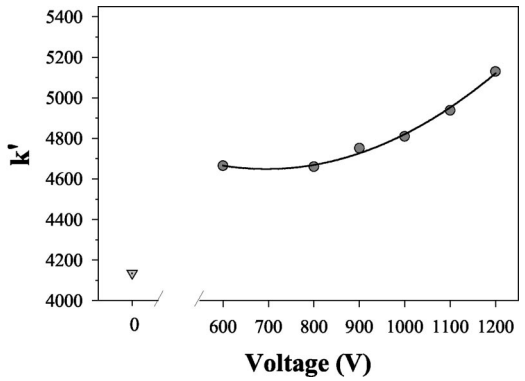

Fig. 7. Parameter k' as a function of the voltage applied to the ceramic plate. The solid line represents the fit to a quadratic function. The data for 0 V are also included (triangle).

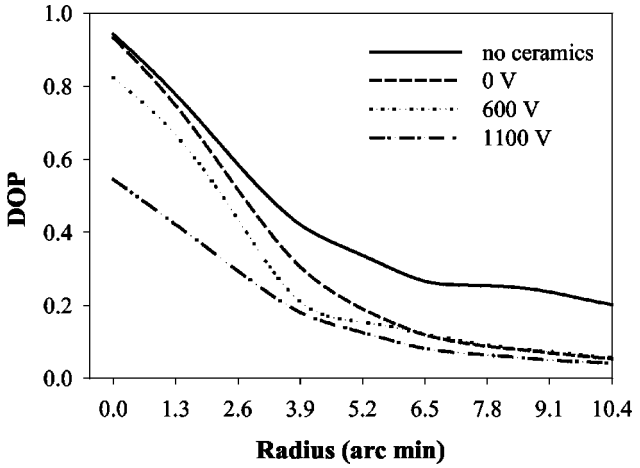

Fig. 8. Values of DOP at different locations along the DP image for different scattering levels.

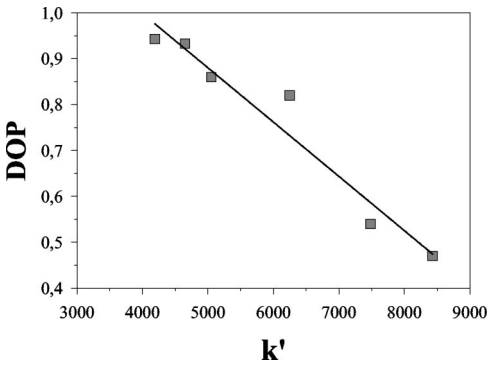

Fig. 9. DOP values at 2.6 arc min central part of the image versus parameter k' for different scattering levels.

4. CONCLUSIONS

A new polarimetric method for estimating objectively the relative amount of light scattering in an optical system has been described. It is based on measuring the DOP of the light in the central part of the DP images formed through the system under test. We studied the accuracy of this procedure in a system that included a PLZT ceramic plate that was able to generate a variable amount of scattered light as a function of the voltage applied. These changes in the scattering levels are independent of the influence of the aberrations, so the effects of the scattering itself can be analyzed in depth.

Our results have shown that the DOP measured at the central part of the DP image is linearly correlated with the increase of the amount of light in the tails of the im-

age, which in turn is directly related to the scattering increase. This indicates that the DOP should be a useful tool to measure and quantify the levels of scattering in optical media.

The quantification of scattering is important in those applications where the image degradation needs to be minimized. Depending on the application, the degradation caused by aberrations and–or scattering has been overcome by means of different approaches, from adaptive optics[18,19] and time-resolving imaging[20] to optical coherence methods.[21] In addition, polarization-difference imaging techniques have been shown to enhance the PSF and to improve the detection of targets embedded in scattering media.[22] However, although polarization has been used to improve contrast in optical imaging through scattering media, as far as we know the relative amount of scattering has never been directly quantified by use of a polarimetric parameter in the sense demonstrated by the approach described here.

A particularly interesting application of this methodology will be in visual optics to estimate intraocular scattering. This may be an alternative to the current subjective clinical observations of cataracts and losses of transparency in the ocular media that are especially prevalent in older people. The study of halos and glare effects following refractive surgery could also be an application of this kind of technique in a clinical environment. Finally, the present method could improve the diagnosis of retinal pathologies directly associated with depolarizing effects.

ACKNOWLEDGMENT

This work was supported by the Ministerio de Ciencia y Tecnología, Spain, grant BFM2001-0391 to P. Artal.

Corresponding author Juan M. Bueno's e-mail address is bueno@um.es; fax, 34968363528.

*Permanent address, Institute of Solid State Physics, University of Latvia, LV-1063 Riga, Latvia.

REFERENCES

1. M. J. Allen and J. J. Vos, "Ocular scattered light and visual performance as a function of age," Am. J. Optom. Physiol. Opt. **44**, 717–727 (1967).
2. J. K. Ijspeert, P. W. de Waard, T. J. van der Berg, and P. T. de Jong, "The intraocular stray-light function in 129 healthy volunteers; dependence on angle, age and pigmentation," Vision Res. **30**, 699–707 (1990).
3. G. Rousset, "Wavefront sensing," in *Adaptative Optics for Astronomy*, D. M. Alloin and J.-M. Mariotti, eds. (Kluwer Academic, Dordrecht, the Netherlands, 1994), Vol. 423, pp. 115–138.
4. J. Liang, B. Grimm, S. Goeltz, and J. F. Bille, "Objective measurement of wave aberrations of the human eye with the use of a Hartmann–Shack wave-front sensor," J. Opt. Soc. Am. A **11**, 1949–1957 (1994).
5. I. Iglesias, E. Berrio, and P. Artal, "Estimates of the ocular wave aberration from pairs of double pass retinal images," J. Opt. Soc. Am. A **15**, 2466–2476 (1998).
6. W. S. Bickel and W. M. Bailey, "Stokes, Mueller matrices, and polarized light scattering," Am. J. Phys. **53**, 468–478 (1985).
7. F. Delplanke, "Automated high-speed Mueller matrix scatterometer," Appl. Opt. **36**, 5388–5395 (1997).
8. A. H. Hielscher, A. A. Eick, J. R. Mourant, D. Shen, J. P. Freyer, and I. J. Bigio, "Diffuse backscattering Mueller matrices of highly scattering media," Opt. Express **1**, 441–453 (1997).
9. B. D. Cameron, M. J. Rakovic, M. Mehrübeoglu, G. W. Kattawar, S. Rastegar, L. V. Wang, and G. L. Coté, "Measurement and calculation of the two-dimensional backscattering Mueller matrix of a turbid medium," Opt. Lett. **23**, 485–487 (1998).
10. R. A. Chipman, "Polarimetry," in *Handbook of Optics*, 2nd ed., M. Bass, ed. (McGraw-Hill, New York, 1995), Vol. 2, Chap. 22.
11. J. Santamaría, P. Artal, and J. Bescós, "Determination of the point-spread function of human eyes using a hybrid optical-digital method," J. Opt. Soc. Am. A **4**, 1109–1114 (1987).
12. P. Artal, I. Iglesias, N. López-Gil, and P. G. Green, "Double-pass measurements of the retinal-image quality with unequal entrance and exit pupil sizes and the reversibility of the eye's optical system," J. Opt. Soc. Am. A **12**, 2358–2366 (1995).
13. M. Ozolins, I. Lacis, R. Paeglis, A. Sternberg, S. Svanberg, S. Andersson-Engels, and J. Swartling, "Electro-optic PLZT ceramics devices for vision science applications," Ferroelectrics **273**, 131–136 (2002).
14. J. M. Bueno and P. Artal, "Double-pass imaging polarimetry in the human eye," Opt. Lett. **24**, 64–66 (1999).
15. P. M. Prieto, F. Vargas-Martín, S. Goelz, and P. Artal, "Analysis of the performance of the Hartmann–Shack sensor in the human eye," J. Opt. Soc. Am. A **17**, 1388–1398 (2000).
16. R. J. Noll, "Zernike polynomials and atmospheric turbulence," J. Opt. Soc. Am. **66**, 207–211 (1976).
17. J. M. Bueno and J. Jaronski, "Spatially resolved polarization properties for *in vitro* corneas," Ophthalmic Physiol. Opt. **21**, 384–392 (2001).
18. N. Hubbin and L. Noethe, "What is adaptive optics?" Science **262**, 1345–1484 (1993).
19. E. J. Fernández, I. Iglesias, and P. Artal, "Closed-loop adaptive optics in the human eye," Opt. Lett. **26**, 746–748 (2001).
20. G. Indebetouw and P. Klysubun, "Imaging through scattering media with depth resolution by use of low-coherence gatings in spatiotemporal digital holography," Opt. Lett. **25**, 212–214 (2000).
21. J. F. de Boer, T. E. Milner, M. J. C. Van Gemer, and J. S. Nelson, "Two-dimensional birefringence imaging in biological tissue by polarization sensitive optical coherence tomography," Opt. Lett. **22**, 934–936 (1997).
22. M. P. Rowe, E. N. Pugh, Jr., J. S. Tyo, and N. Engheta, "Polarization-difference imaging: a biologically inspired technique for imaging in scattering media," Opt. Lett. **20**, 608–610 (1995).